Molecular Neurobiology (2019) 56:2774–2790
https://doi.org/10.1007/s12035-018-1280-9

Ferulic Acid Rescues LPS-Induced Neurotoxicity via Modulation of the TLR4 Receptor in the Mouse Hippocampus

Shafiq Ur Rehman[1] · Tahir Ali[1] · Sayed Ibrar Alam[1] · Rahat Ullah[1] · Amir Zeb[1] · Keun Woo Lee[1] · Bart P. F. Rutten[2] · Myeong Ok Kim[1]

Received: 27 March 2018 / Accepted: 23 July 2018 / Published online: 30 July 2018

Abstract

Microglia play a crucial role in the inflammatory brain response to infection. However, overactivation of microglia is neurotoxic. Toll-like receptor 4 (TLR4) is involved in microglial activation via lipopolysaccharide (LPS), which triggers a variety of cytotoxic pro-inflammatory markers that produce deleterious effects on neuronal cells. Ferulic acid (FA) is a phenolic compound that exerts antioxidant and anti-inflammatory effects in neurodegenerative disease. However, the manner in which FA inhibits neuroinflammation-induced neurodegeneration is poorly understood. Therefore, we investigated the anti-inflammatory effects of FA against LPS-induced neuroinflammation in the mouse brain. First, we provide evidence that FA interferes with TLR4 interaction sites, which are required for the activation of microglia-induced neuroinflammation, and further examined the potential mechanism of its neuroprotective effects in the mouse hippocampus using molecular docking simulation and immunoblot analysis. Our results indicated that FA treatment inhibited glial cell activation, p-JNK, p-NF_KB, and downstream signaling molecules, such as iNOS, COX-2, TNF-α, and IL-1β, in the mouse hippocampus and BV2 microglial cells. FA treatment strongly inhibited mitochondrial apoptotic signaling molecules, such as Bax, cytochrome C, caspase-3, and PARP-1, and reversed deregulated synaptic proteins, including PSD-95, synaptophysin, SNAP-25, and SNAP-23, and synaptic dysfunction in LPS-treated mice. These findings demonstrated that FA treatment interfered with the TLR4/MD2 complex binding site, which is crucial for evoking neuroinflammation via microglia activation and inhibited NF_KB likely via a JNK-dependent mechanism, which suggests a therapeutic implication for neuroinflammation-induced neurodegeneration.

Keywords Microglia · LPS · TLR4 · Neuroinflammation · Neurodegeneration · ROS · Synaptic dysfunction

Abbreviations

CNS	Central nervous system
PBS	Phosphate-buffered saline
NF_KB	Nuclear factor kappa B
TNF-α	Tumor necrosis factor-alpha
iNOS	Inducible nitric oxide synthase
COX-2	Cyclooxygenase-2
p-JNK	Phospho-C-jun N-terminal Kinase
PARP-1	Poly[ADP-ribose] polymerase 1
TRITC	Tetramethylrhodamine isothiocyanate
FITC	Fluorescein isothiocyanate
DG	Dentate gyrus
CA1	Cornu Ammonis
PSD-95	Post-synaptic density-95
SNAP23	Synaptosomal-associated protein 23
SD	Standard deviation
i.p.	Intraperitoneally
NAOH	Sodium hydroxide
IKK	IkB kinases
Iba-1	Ionized calcium-binding adapter molecule 1
GFAP	Glial fibrillary acidic protein
KMNO4	Potassium permanganate

Electronic supplementary material The online version of this article (https://doi.org/10.1007/s12035-018-1280-9) contains supplementary material, which is available to authorized users.

✉ Myeong Ok Kim
mokim@gsnu.ac.kr

[1] Division of Life Sciences and Applied Life Science (BK 21plus), College of Natural Sciences, Gyeongsang National University, Jinju 52828, Republic of Korea

[2] Department of Psychiatry and Neuropsychology, School for Mental Health and Neuroscience (MHeNS), Faculty of Health, Medicine and Life Sciences, Maastricht University, European Graduate School of Neuroscience (EURON), Maastricht, The Netherlands

Introduction

Activated glial cells are the hallmark of neuroinflammation and various neurodegenerative diseases, including Parkinson's disease (PD) and Alzheimer's disease (AD) [1, 2]. Activated microglia in the central nervous system (CNS) trigger a variety of cytotoxic pro-inflammatory markers and reactive oxygen species (ROS), which produce detrimental effects on CNS [3–5]. Activation of these inflammatory mediators boosts neuronal injury via a receptor-dependent apoptotic pathway [6, 7]. Toll-like receptors are involved in lipopolysaccharide (LPS)-induced microglial activation, which activates nuclear factor kappa B (NF_KB). NF_KB is a critical transcription factor for the induction of inflammatory mediators. A previous study suggested the involvement of toll-like receptor 4 (TLR4) in association with myeloid differentiation factor 2 (MD-2) for LPS physiological recognition [8, 9]. The nuclear translocation of NF_KB involves the phosphorylation and degradation of NF_KB-bound IkB via IKK phosphorylation, which results in the expression of pro-inflammatory mediators, including cyclooxygenase-2 (COX-2), inducible nitric oxide synthase (iNOS), and cytokines [10]. Another study suggested that the phospho-C-jun N-terminal Kinase (JNK)/mitogen-activated protein kinases (p38MAPK) signaling pathway contributed to neuronal cell death during inflammatory processes [11]. Pro-inflammatory cytokines exhibit many significant physiological functions in the CNS. However, the overproduction and deregulation of pro-inflammatory cytokines from active microglia contribute to chronic neurodegenerative diseases, including AD, PD, and multiple sclerosis, and acute neurodegenerative conditions, such as stroke and traumatic brain injury [12–15]. A recent study demonstrated that the overproduction of pro-inflammatory cytokines leads to synaptic dysfunction and neuronal cell death [16].

Lipopolysaccharide (LPS) plays an important role in the pathogenesis of the inflammatory response and microglial activation [17]. LPS triggers mitogen-activated protein kinases (MAPKs), which are involved in the release of cytotoxic factors, including nitric oxide (NO), COX-2, interleukin-6 (IL-6), and interleukin-1 beta (IL-1β) [18, 19]. Several studies demonstrated that LPS activated the NF_KB-regulated immune response via the MAPK signaling pathway [20, 21]. LPS induces an overproduction of ROS, which leads to microglial activation and the induction of a neuroinflammatory process that further contributes to neuronal damage and neurodegenerative disorders [22, 23]. Therefore, the inhibition of microglial activation and the overproduction of pro-inflammatory mediators and cytokines is a potential neuroprotective treatment strategy.

Ferulic acid (FA) is a well-known phenolic compound that is abundant in fruits, cereals, coffee, and vegetables, and it may exert beneficial effects against diabetes, cardiovascular disease, cancer, and neurodegenerative diseases [24, 25]. FA exhibits free radical-scavenging, antioxidant, and anti-inflammatory properties in various neurodegenerative diseases and neuroprotective activity against focal cerebral ischemia via modulation of apoptotic protein expression and regulation of the inflammatory reaction [26–28]. FA also prevented β amyloid-induced toxicity in vivo [29].

The effect of FA on microglia-mediated neuroinflammation via activation of TLR4 receptor signaling is not known. The present study investigated the effects of FA on LPS-induced microglial activation in mouse hippocampus and BV2 microglial cells. We report for the first time that FA exerted its neuroprotective effects via modulation of TLR4 interaction sites that are crucial for activation of the neuroinflammatory cascade and via a JNK-dependent mechanism in microglia cells. FA may interfere with the TLR4-MD2 complex, which is required for the activation of microglia-mediated neuronal inflammation and neurodegeneration.

Materials and Methods

Lipopolysaccharide and FA were purchased from Sigma-Aldrich Chemical Co. (St. Louis, MO, USA). SP600125 was purchased from Santa Cruz Biotechnology, USA.

Microglial Cell Culture Treatment

BV2 cells were kindly provided by Dr. I. W. Choi (Inje University, South Korea) and grown in DMEM supplemented with 10% fetal bovine serum (FBS) and antibiotics (penicillin/streptomycin). Cells were maintained in an incubator (37 °C) with 5% CO_2. Cells were preincubated with FA and inhibitors for 2 h in all experiments followed by post-incubation with LPS for 24 h. The following cell treatments were used: (1) control (C) incubated in DMEM, (2) FA treatment (10–100 μM), (3) LPS treatment 1 μg/ml, (4) LPS plus FA (10 and 100 μM) treatment, (5) LPS plus FA (100 μM) treatment, (6) LPS plus TAK242 (2 μM) treatment, and (7) LPS plus SP600125 (20 μM) treatment. Western blot analysis was performed 24 h after treatment.

Animals and Drug Treatments

Male C57BL/6N mice (25–30 g, 8 weeks of age) were purchased from Samtako Bio (Korea) and housed under a 12/12-h light and dark cycle at 23 °C and 60 ± 10% humidity. Food and water were provided ad libitum. Mice were acclimatized for 1 week and randomly assigned to four groups ($n = 15$ in each group). FA treatment was started 4 days prior to and

continued throughout the 7 days of LPS injection. The treatment schedule was as follows:

- Control mice (C) treated with saline as a vehicle for 7 days
- Mice treated with LPS (0.33 mg/kg, i.p.)
- Mice treated with LPS (0.33 mg/kg, i.p.) plus FA (20 mg/kg)
- Mice treated with FA alone (20 mg/kg)

FA was initially dissolved in 1% dimethyl sulfoxide (DMSO), diluted with saline and orally administered to mice. Figure 9a describes the treatment schedule. All experimental procedures and techniques used in this study were performed in accordance with the rules established by the animal ethics committee of the Division of Applied Life Sciences, Department of Biology, Gyeongsang National University, South Korea.

Protein Extraction

Mice were killed after treatment, and the brains were removed ($n = 8$ each group). The cortex and hippocampus were carefully dissected and frozen at − 80 °C. The hippocampus tissue was homogenized in 0.2 M phosphate-buffered saline (PBS) containing a protease inhibitor cocktail followed by centrifugation. Proteins were stored at − 80 °C for further analysis.

Western Blot Analysis

Western blot analysis was performed as previously described [30]. Briefly, the protein concentration was determined using a Bio-Rad protein assay kit (Bio-Rad Laboratories, CA, USA) according to the manufacturer's instructions. An equal volume of protein (20–25 μg) was electrophoresed in 4–12% Bolt™ Mini Gels (Novex; Life Technologies, Kiryat Shmona, Israel). Membranes were blocked in 5% (*w*/*v*) skim milk to reduce nonspecific binding, incubated with primary antibodies overnight at 4 °C, and incubated with horseradish peroxidase-conjugated secondary antibodies. Proteins were detected using ECL detecting reagents. Loading was normalized using an antibody against beta-actin.

Antibodies

Table 1 lists the antibodies used for immunoblot and immunofluorescence (Supp. Fig 1).

Tissue Collection and Sample Preparation

Male mice ($n = 7$ each group) were perfused transcardially with saline followed by ice-cold 4% paraformaldehyde. Brains were post-fixed in 4% paraformaldehyde for 72 h and transferred to sucrose (20%) for 48 h. Brains were frozen in OCT compound (AO USA) and sectioned at a thickness of 14 μm using a cryostat (Leica, Germany). Sections were thaw-mounted on ProbeOn Plus Charged Slides (Fisher, Rockford, IL, USA). Slides were stored at − 80 °C for further immunohistological study.

Immunofluorescence Staining

The hippocampus and cortical regions were selected for immunofluorescence analyses. Sections were washed twice (8–10 min) in 0.1 M PBS solution and incubated with a blocking solution (0.1% Triton X-100 and 2% normal goat/rabbit serum in 0.1 M PBS) for 60 min at room temperature. The slides were incubated (overnight) at 4 °C in primary antibodies: anti-GFAP, anti-TNF-α, anti-NF_KB, anti-caspase-3, and anti-SNAP-23 (Santa Cruz Biotechnology, USA) diluted 1:100 in blocking solution. The sections were incubated (90 min) with tetramethylrhodamine isothiocyanate (TRITC) and fluorescein isothiocyanate (FITC)-labeled (1:100) secondary antibodies (Santa Cruz Biotechnology, USA). The sections were mounted, incubated with 4′,6′-diamidino-2-phenylindole (DAPI) for 8–10 min, and covered with glass coverslips using mounting medium. A confocal laser-scanning microscope (Flouview FV 1000 MPE) was used to examine the immunofluorescence.

Measurement of ROS Production

ROS production was measured using the DCF-DA assay, as previously described [31] with some modification.

Fluoro-Jade B Staining

Fluoro-Jade B (Cat# AG310, Millipore, USA) staining was performed as previously described (Badshah et al. 2016b). Briefly, hippocampal and cortical tissue sections from the treated mouse groups were air-dried overnight, washed twice with PBS for 10 min, and immersed in a solution of NaOH (1% *w*/*v*) and ethanol (80% *v*/*v*) for 5 min. The slides were washed with ethanol (70% *v*/*v*) for 2 min followed by a wash with distilled water. Slides were immersed in a $KMNO_4$ solution (0.06% *w*/*v*) for 10 min and washed with distilled water. The slides were transferred to FJB solution (0.01% *v*/*v*) containing acetic acid (0.1%) for 15 min. Slides were washed 3 times for 1 min with distilled water and placed in an incubator for 5 min to dry at a warm temperature. Glass coverslips were mounted in DPX (nonfluorescent mounting medium). Images were captured using confocal laser scanning microscopy (Flouview FV 1000 MPE).

Determination of Lipid Peroxidation

A lipid peroxidation (LPO) quantification assay was performed as previously described with some modification [32]. Free malondialdehyde (MDA) in the hippocampi of LPS- and

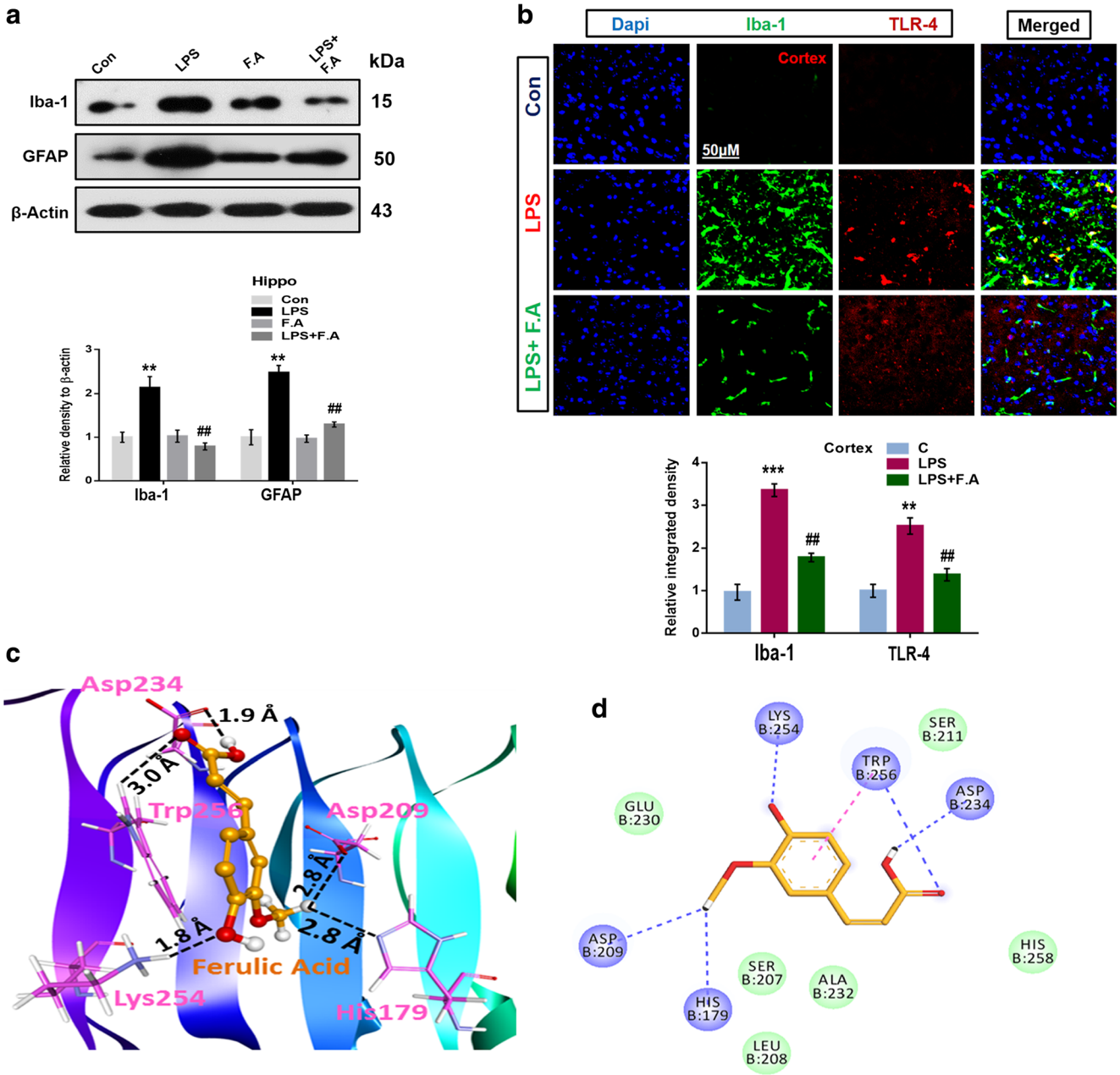

Fig. 1 Ferulic acid inhibited glial cell activation and the TLR4-mediated signaling pathway in the LPS-treated mouse hippocampus. **a** Representative immunoblots showing the expression levels of Iba-1 and GFAP probed with specific antibodies. Mice were pretreated with FA for 4 days followed by LPS treatment and oral FA treatment for 7 days ($n = 7$ mice/group). **b** Representative immunofluorescence analysis of Iba-1 and TLR4 colocalization in cortex region treated with LPS and LPS plus FA ($n = 7$ mice/group). **c** FA is shown as a ball and stick model. Golden, red, and white colors represent carbon, oxygen, and hydrogen, respectively. Ferulic acid-interacting residues of TLR4 are depicted as purple-colored thin sticks, while hydrogen bonds are displayed as black dashed lines. **d** 2D representation of molecular interactions of TLR4-FA complex. Black-circled green discs show hydrogen bond formation, while light dark spheres portray TLR4 residues that are involved in van der Waals interactions. Magnification ×10. Statistical analysis was done using one-way ANOVA followed by post hoc analysis. $^{**}P < 0.01$ vs. control group; $^{\#\#}P < 0.01$ vs. LPS group

FA-treated mouse groups was assessed using a thiobarbituric acid-reactive substance (TBARS) assay kit (BioVision, USA) according to the manufacturer's instructions. Absorbance was measured using a microplate reader at 532 nM. The MDA content is expressed as nanomoles per milligram of protein in the tissue homogenate.

Behavioral Analysis

Mouse behavior was assessed using the Morris water maze (MWM) test ($n = 15$). The MWM apparatus was a circular water tank (100 cm in diameter and 40 cm in height) filled with 25 °C water to a depth of 15.5 cm. The water was made

opaque using white ink. A platform 10 cm in diameter and 14.5 cm in height (i.e., 1 cm below the water surface) was placed hidden in the middle of one quadrant of the tank. Mice received four training periods/day for four consecutive days prior to treatment, followed by 4 days of rest. Mice were given 60 s for each trial to find the platform, and mice were allowed to remain on the platform for 30 s. The latency to escape from the water was calculated for four consecutive days. The probe test was performed on day 5 with the hidden platform removed from the maze, and the mice were allowed to swim for 60 s. The latency to the platform, time spent in the target and three nontarget quadrants, and number of crossings over the platform were calculated. Mice were sacrificed after the probe test for further biochemical and histological analyses. A video tracking system (SMART, Panlab Harvard Apparatus, Bioscience Company, USA) was used to record and quantitate mouse swimming.

Molecular Docking of Ferulic Acid in TLR4

Genetic Optimization of Ligand Docking (GOLD v5.2.2) [33] was used to dock FA into its binding site on TLR4. The X-ray structure of TLR4 (PDB ID 2Z65) with 2.7 Å resolution was obtained from the RCSB Protein Data Bank (www.rcsb.org) [34, 35]. All water molecules, heteroatoms, co-crystallized protein, and nonprotein structures were removed from the TLR4 structure prior to docking, and hydrogen atoms were added in Discovery Studio (v4.5). The suitable binding site for small molecules on TLR4 was identified from previously published literature [34, 36, 37]. The binding site was carefully defined as the area within 9 Å from the most crucial residues Ser183 and Asp209 of TLR4 and Arg106 of MD2 [34]. A total of 50 conformational poses of FA were created using the genetic algorithm (GA) module implanted in GOLD. The piecewise linear potential (ChemPLP) and Astex statistical potential (ASP) scores were used as default scoring and rescoring functions, respectively, to evaluate the best pose orientation [38]. The best-oriented pose was selected on the basis of the highest ChemPLP and ASP scores and the hydrogen bond interactions with TLR4 residues crucial for interaction with MD2. The docking results were analyzed using Discovery Studio and Visualization of Molecular Dynamics (VMD) software.

Statistical Analysis

Scanned immunoblots were analyzed using densitometry in Sigma gel software (SPSS Inc., Chicago, IL). ImageJ software was used to analyze immunohistological images. The values were calculated as the means ± SEM and analyzed using one-way ANOVA followed by post hoc analysis. Statistical analyses were performed using GraphPad Prism 5 software. $P < 0.05$ was considered statistically significant. $*P < 0.05$, $**P < 0.01$, and $***P < 0.01$ represent significant differences between control and LPS; $\#P < 0.05$, $\#\#P < 0.01$, and $\#\#\#P < 0.01$ represent significance differences between LPS and LPS plus FA, TAK242, and SP600125, respectively.

Results

Ferulic Acid Inhibited LPS-Induced Neuroinflammation via a TLR4-Mediated Signaling Pathway in the Mouse Hippocampus

Several studies reported LPS-induced microglia and astrocyte activation in animal models and cell cultures [39]. We examined microglia and astrocyte activation in the mouse hippocampus using Western blot analysis to investigate whether FA inhibit glial activation in LPS-treated mouse hippocampus. Our results indicated a higher level of Iba-1 (a marker of activated microglia) and GFAP (a marker of activated astrocytes) in the hippocampi of mice treated with LPS (0.33 mg/kg, i.p.) compared to the saline-treated group. FA (20 mg/kg/day) pretreatment significantly ($P < 0.01$) reduced GFAP and Iba-1 levels in the mouse hippocampus compared to the group treated with LPS alone (Fig. 1a). Brain tissues were examined using immunofluorescence techniques to analyze active microglia and TLR4 activation in LPS-treated mice. Our findings revealed an increase in the number of active microglia and TLR4, which colocalized in the cortical region of the LPS-treated mice compared to the saline-treated mice. However, microglia activation and increased TLR4 expression were significantly abolished with LPS plus FA treatment (Fig. 1b), which suggests that FA treatment protects the mouse brain against neuroinflammation-mediated neurotoxicity. A previous study demonstrated that TLR4 formed a heterodimer with myeloid differentiation factor 2 (MD2). This complex specifically recognizes lipopolysaccharide (LPS) and induces TLR4-mediated stimulation [36, 40]. FA suppressed LPS-induced TLR4 activation in our in vivo analysis. Therefore, we examined the predicted binding of FA with TLR4 using molecular docking simulation. FA docking on TLR4 exhibited a highest ChemPLP score of 51.28 and highest ASP score of 20.61. The docking results demonstrated that FA targeted the crucial binding site of TLR4 and disrupted TLR4-MD2 complex formation. The 3D structural analysis of the TLR4-FA complex demonstrated that FA was sandwiched between Asp209 and Trp256 and formed polar interactions with these sites. The detailed molecular interaction analysis suggested that FA established polar interactions with TLR4 residues. Our docking results revealed that the methoxy group of FA

formed hydrogen bonds with the side chain oxygen of Asp209 and the Nε of His179, with bond distances of 2.8 Å each (Fig. 1c). Asp209 plays a critical role in the polar interaction of TLR4 and MD2 to form a stable complex. Therefore, we claim that the hydrogen bond formation of Asp209 with FA may disrupt TLR4-MD2 complex. This mechanism of TLR4 inactivation was reported previously [34, 37, 41]. Our docking analysis also predicted a hydrogen bond interaction between the hydroxyl group of FA and the carbonyl oxygen of Asp234 in TLR4 with a bond distance of 1.9 Å (Fig. 1c). The polar interaction of Asp234 with a small molecule inhibitor played an essential role in disruption of the TLR4-MD2 complex [41]. Our results also predicted hydrogen bond formation between the phenolic oxygen of FA with the side chain of Lys254 and carbonyl oxygen of FA with the side chain of Trp256 with bond distances of 1.8 and 3.0 Å, respectively (Fig. 1e). These newly identified hydrogen bond interactions likely further stabilize FA in the TLR4 binding site. We also observed π-π stacked interactions between the phenolic group of FA and the indole group of the nonpolar side chain of Trp256. Other residues formed van der Waals interactions are depicted in Fig. 1d. The polar interactions remained the essential driving forces of the TLR4-MD2 complex. Therefore, our docking results suggest that FA disrupts the TLR4-MD2 complex via formation of polar interactions with TLR4. The topological orientation (Fig. S1) of FA revealed that it was sandwiched between the MD2-binding residues Asp209 and Trp256 of TLR4 [41]. We proposed that the disruption of the TLR4-MD2 complex by FA eradicated the LPS binding cavity and abolished LPS toxicity in treated mouse brains. We examined the immunoreactivity of the activated JNK and GFAP using confocal microscopy. The results demonstrated that active JNK and GFAP immunoreactivity was higher in LPS-treated mouse hippocampal and cortical regions, and FA treatment significantly abolished the LPS-induced increase (Fig. 2a, b).

We examined LPS-evoked TLR4 expression in microglial cells and the downstream signaling molecules involved in neuroinflammation-mediated toxicity in the brain. Western blot results clearly demonstrated higher expression levels of TLR4 and downstream signaling molecules, including p-JNK, p-IKK-β, and p-NF_KB, in the hippocampi of mice treated with LPS compared to the saline-treated group (Fig. 3a, b). Notably, FA treatment significantly attenuated these inflammatory mediators via inhibition of TLR4 in LPS-treated mice. These findings were supported in the immunofluorescence staining of the nuclear translocation of NF_KB in LPS-treated mice and FA inhibition of translocation in hippocampal CA1 and DG regions of mice (Fig. 3c). These results suggest that FA protected against neuronal toxicity via modulation of microglia-induced neuroinflammatory activity via the TLR4 signaling pathway in the mouse brain.

Ferulic Acid Inhibited Upregulated Inflammatory Markers in BV2 Cells

TLR4 binding to LPS initiates an inflammatory cascade in microglia that involves NF_KB activation [39, 42, 43]. We investigated the TLR4-mediated expression of p-JNK, NF_KB, and inflammatory mediators, including iNOS and TNF-α proteins, in LPS-treated BV2 cells and the possible reversal effects of FA against these inflammatory mediators in a concentration-dependent manner. Western blot demonstrated that LPS (1 μg/ml) treatment increased p-JNK, NF_KB, iNOS, and TNF-α levels. However, FA (10 and 100 μM) significantly inhibited the production of these neuroinflammatory mediators in a concentration-dependent manner (Fig. 4a–e). FA (100 μM) was more effective. These observations suggest that FA exhibited a potent anti-inflammatory effect against LPS-induced neuroinflammation via a microglial TLR4-mediated signaling pathway.

Ferulic Acid Treatment Inhibited TLR4-Mediated Inflammatory Signaling in BV2 Microglial Cells

Figure 5a shows that the exposure of BV2 cells to LPS (1 μg/ml) increased TLR4 expression. However, FA (100 μM) treatment significantly reversed the increased expression of TLR4. Treatment of LPS-treated BV2 cells with the TLR4-specific inhibitor TAK242 also inhibited TLR4 activation in a similar manner as FA. We investigated the TLR4 downstream signaling molecules, including p-JNK and p-NF_KB, and TAK242 (2 μM) and FA (100 μM) significantly inhibited these molecules. Our results suggest that FA exhibited potent anti-inflammatory effects via a TRL-4-mediated signaling pathway. Previous studies reported that MAPK regulated p-NF_KB activation. Therefore, we investigated the effects of FA treatment on p-JNK and p-NF_KB in BV2 microglial cells. Notably, FA treatment inhibited p-NF_KB activation in a JNK-dependent manner. Figure 5b shows that FA (100 μM) and SP600125 (20 μM) significantly inhibited p-NF_KB in a JNK-dependent manner. Therefore, FA treatment inhibited the inflammatory response via TRL-4 inhibition and inhibition of p-NF_KB via a JNK-dependent mechanism.

Ferulic Acid Treatment Inhibited the Inflammatory Response in the Mouse Hippocampus

We observed the activation of neuroinflammatory mediators in the mouse hippocampus to confirm the TLR4-mediated inflammatory response. Our results clearly demonstrated an increase in the activation of inflammatory mediators, including iNOS, COX-2, TNF-α, and IL-1β, in the LPS-treated mouse hippocampus compared to saline-treated control mice. However, FA treatment significantly inhibited the increased expression of these inflammatory mediators in the mouse

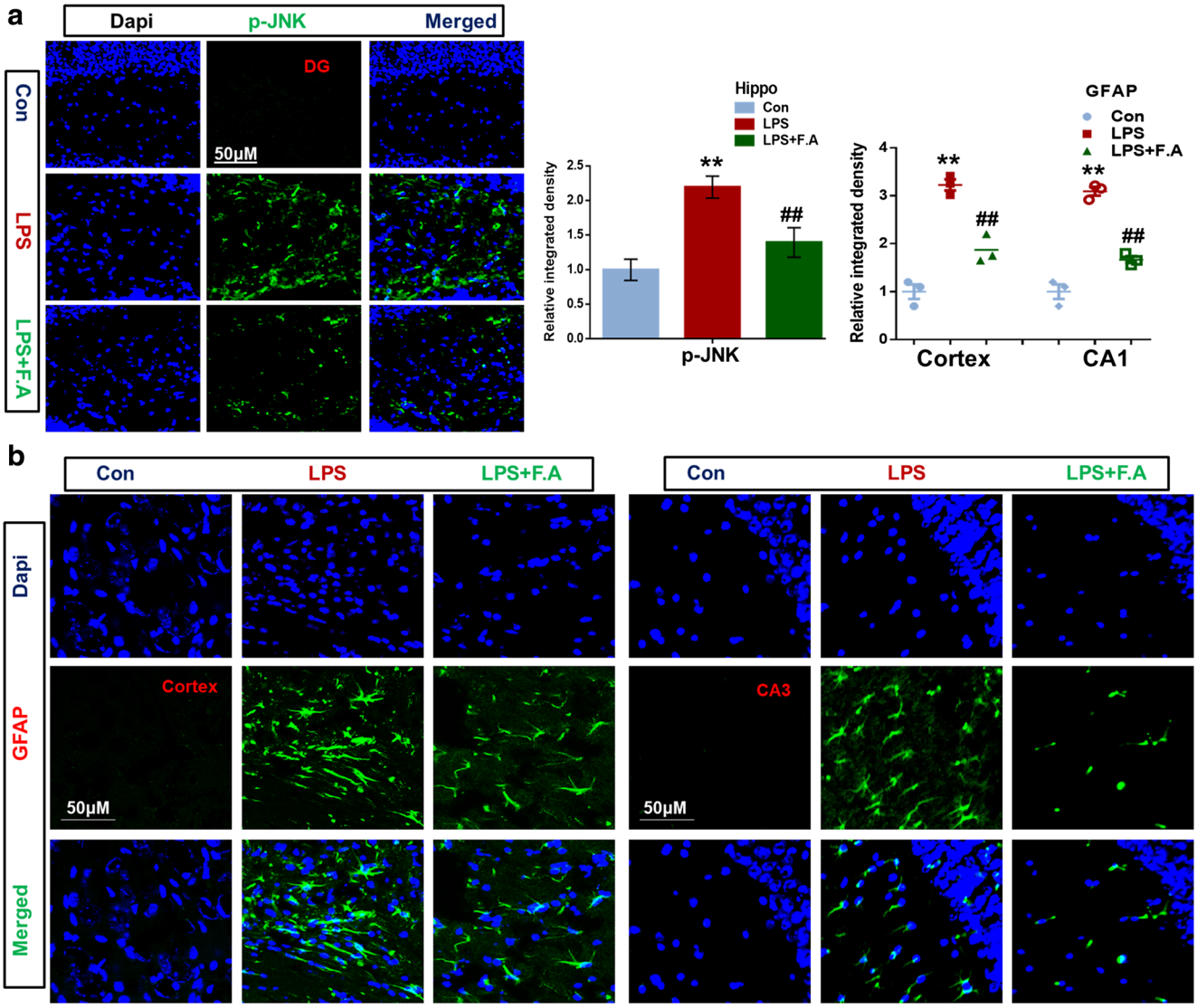

Fig. 2 Ferulic acid abolished the activation of JNK and astrocytes in the LPS-treated mouse cortex and hippocampus. **a** Immunofluorescence results indicating p-JNK in the hippocampal DG region among the treated groups. **b** The active astrocytes immunostained with GFAP (marker of astrocytes). ImageJ software was used to quantify the immunohistological analysis ($n = 7$ mice/group). Magnification ×10. Statistical analysis was done using one-way ANOVA followed by post hoc analysis. $^{**}P < 0.01$ vs. control group; $^{\#\#}P < 0.01$ vs. LPS group

hippocampus (Fig. 6a). The immunofluorescence analysis of TNF-α further supported these findings. Our Western blot results revealed that increased TNF-α levels were observed in the DG and CA3 regions of LPS-treated mice compared to saline-treated mice. Notably, FA significantly reduced TNF-α levels in the abovementioned regions compared to mice treated with LPS alone (Fig. 6b).

Ferulic Acid Attenuated LPS-Induced Oxidative Stress in the Mouse Hippocampus

Oxidative stress is a hallmark of various neurodegenerative disorders, including AD and PD. Elevated ROS concentrations produce direct neuronal toxicity and may be implicated in microglia activation via the modification of signaling events [22, 44]. Our results demonstrated that LPS treatment markedly increased the ROS level in the mouse hippocampus compared to saline-treated mice, and FA treatment significantly ($P < 0.01$) attenuated this increase (Fig. 7a). A lipid peroxidation assay revealed an increase in MDA in the LPS-treated mouse group, and FA reduced this increase in the mouse hippocampus ($P < 0.01$) (Fig. 7b). These observations suggest that FA prevented LPS-evoked oxidative stress-induced neuronal toxicity in the mouse brain.

Ferulic Acid Attenuated LPS-Induced Activation of the Mitochondrial Apoptotic Pathway

Debatin and coworkers reported that the mitochondrial apoptotic pathway involves the release of mitochondrial

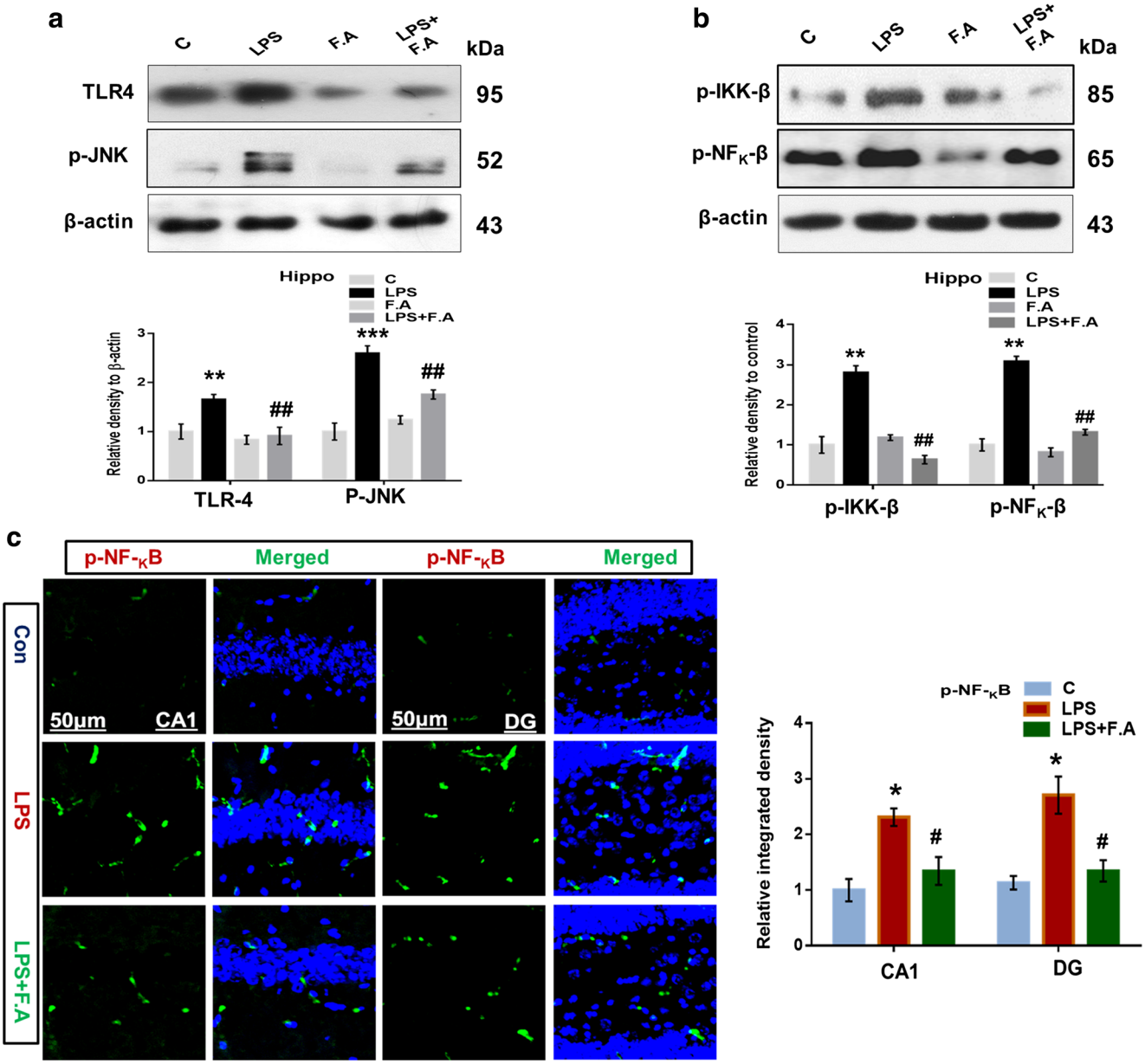

Fig. 3 Ferulic acid inhibited inflammatory mediation in mice hippocampus. **a**, **b** Representative immunoblots and histograms of TLR4, p-JNK, p-IKK-β, and p-NF_KB in experimental groups. **c** Representative photomicrograph of the immunofluorescence analysis of p-NF_KB in experimental groups. For immunoblot analysis, Sigma gel software was used to quantify the bands. The same immunoblots were probed using β-actin as a loading control. **c** The nuclear colocalization of the activated p-NF_KB among the treated groups. Values are expressed in arbitrary units (AU) as the mean ± SEM for the indicated proteins ($n = 8$, each group). ImageJ software was used to quantify the immunohistological analysis ($n = 7$ mice/group). Magnification ×10 for immunofluorescence analysis. Statistical analysis was done via one-way ANOVA followed by post hoc analysis. $^{**}P < 0.01$ vs. control group; $^{\#\#}P < 0.01$ vs. LPS group

cytochrome C, activated caspase-9, caspase-3, and pro-apoptotic Bax [45]. Activated microglia induce neuronal apoptosis via inflammatory cytokine production [46]. C-jun N terminal kinase (JNK) plays a pivotal role in the regulation of neuronal apoptosis [47]. Western blot was performed to investigate the protective effect of FA against the LPS-induced mitochondrial apoptotic pathway. Our findings revealed that LPS administration increased the levels of cytochrome C release, cleaved caspase-3, cleaved PARP-1, and Bax compared to the saline-treated mouse group. However, the increased levels of the apoptotic markers were obviously rescued in FA-treated mice (Fig. 7c). We examined the increased expression of caspase-3 using immunofluorescence. Figure 7d illustrates the increased caspase-3 levels in the LPS-treated mouse hippocampal CA3 region and cortex. FA treatment significantly lowered caspase-3 immunoreactivity in the hippocampus and cortex. We also observed an increase in pro-apoptotic Bax levels in BV2 microglia cells following LPS

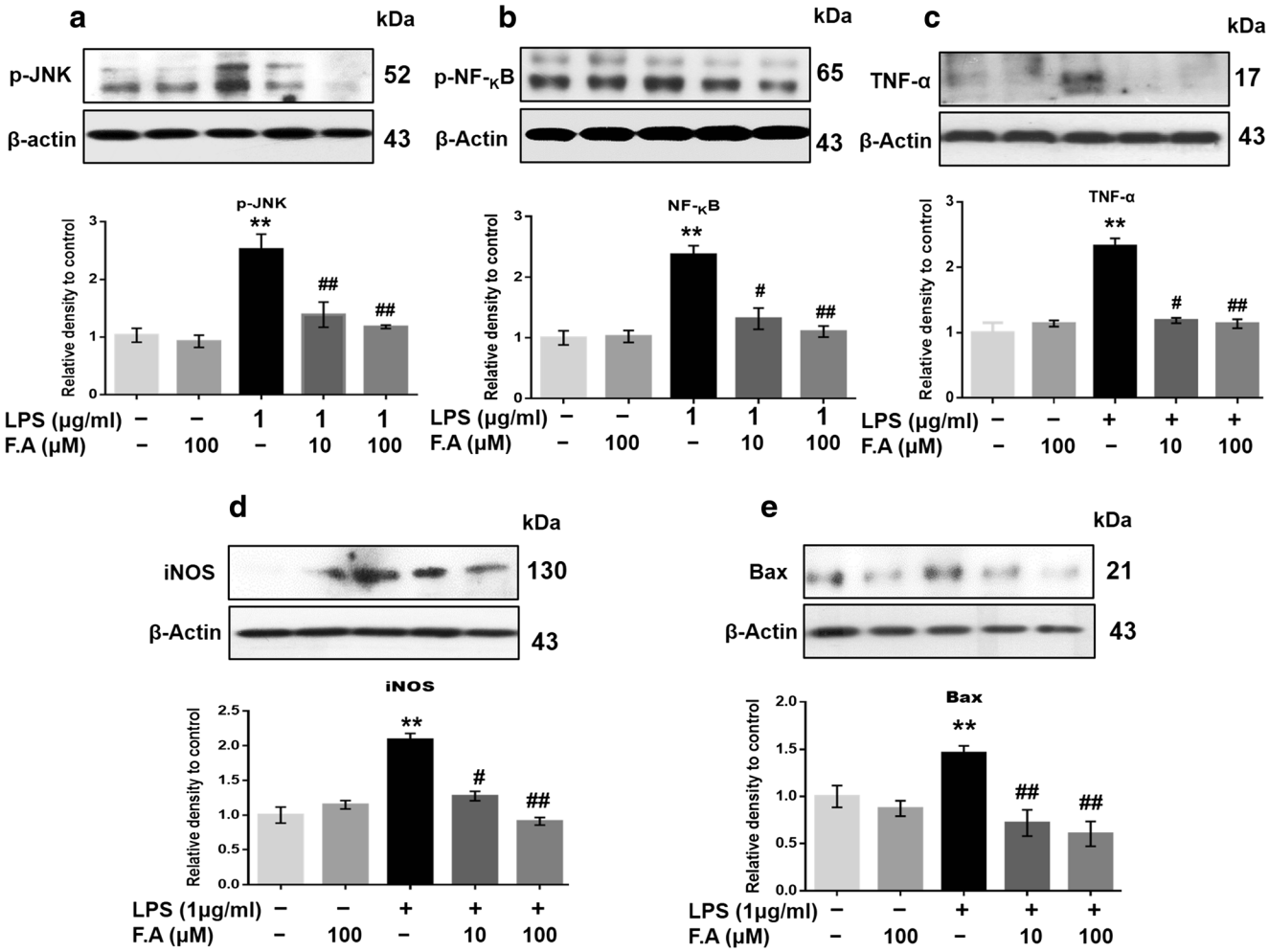

Fig. 4 Ferulic acid attenuated the JNK/NF_KB inflammatory signaling pathway and apoptosis in LPS-stimulated BV2 microglia cells. **a** Representative Western blots and histograms of p-JNK, p-NF_KB, iNOS, TNF-α, and Bax in the LPS-treated and FA-treated groups. The same immunoblots were probed using β-actin as a loading control. Values are expressed in arbitrary units (AU) as the mean ± SEM for the indicated proteins. Statistical analysis was done using one-way ANOVA followed by post hoc analysis. $*P < 0.05$, $**P < 0.01$ vs. control group; $\#P < 0.05$, $\#\#P < 0.01$ vs. LPS group

stimulation. However, FA (10 and 100 μM) significantly reduced the increased Bax levels in BV2 microglial cells (Fig. 4e), which suggests an anti-apoptotic activity of FA in microglia-induced apoptosis in the mouse brain.

Ferulic Acid Inhibited LPS-Induced Neurodegeneration in the Mouse Hippocampus

FJB staining was performed to examine dead neuronal cells. Our histological results revealed an increase in FJB-positive neuronal cells (dead cells) in the cortex and hippocampal CA3 region following LPS administration compared to the saline-treated mouse group. FA and LPS co-treatment significantly reduced the number of damaged neurons in the abovementioned regions of the mouse brain, which suggests that FA was protective against neuroinflammation-induced neurodegeneration in the mouse brain (Fig. 7e).

Ferulic Acid Protected Against Synaptic Marker Loss in LPS-Treated Mouse Hippocampus

The neuroinflammatory processes via microglia activation contributes to several neurodegenerative diseases [48, 49]. Previous research demonstrated that cytokine administration or other immunogenic stimuli, particularly LPS, impaired hippocampus-dependent memory [50, 51]. We examined the effect of FA on the LPS-induced deregulation of synaptic proteins using Western blot. Our results demonstrated that the expression of memory-related proteins, including synaptophysin, SNAP-25, PSD-95, and SNAP-23, significantly ($P < 0.01$) declined in the LPS-treated mouse hippocampus compared to the saline-treated group, and FA treatment reversed these effects and effectively increased the expression levels of synaptic proteins and rescued neuronal dysfunction in the mouse group treated with LPS plus

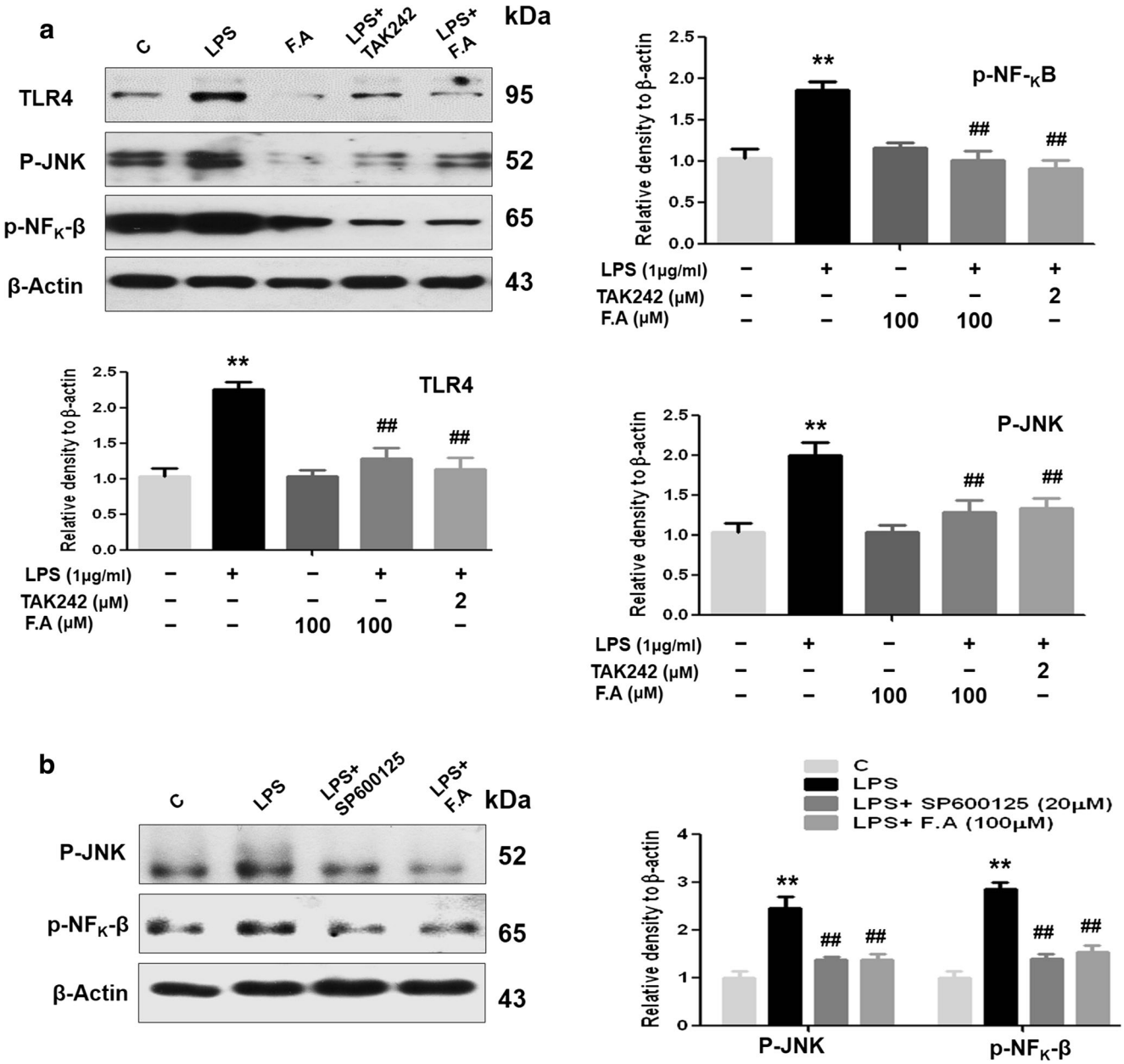

Fig. 5 Effect of ferulic acid on the TLR4-mediated signaling pathway in BV2 microglial cells. **a** Given are the representative Western blots and histograms of TLR4, p-JNK, and p-NF_KB in LPS-treated BV2 cells. BV2 cells were incubated with FA (100 μM) and TAK242 (2 μM) for 2 h and then stimulated with LPS (1 μg/ml) for 24 h. **b** Representative Western blots and histograms of p-JNK and p-NF_KB in LPS-treated BV2 cells. BV2 cells were incubated with FA (100 μM) and SP600125 (20 μM) for 2 h and then stimulated with LPS (1 μg/ml) for 24 h. The same immunoblots were probed using β-actin as a loading control. Values are expressed in arbitrary units (AU) as the mean ± SEM for the indicated proteins. Statistical analysis was done using one-way ANOVA followed by post hoc analysis. $^{**}P < 0.01$ vs. control group; $^{\#\#}P < 0.01$ vs. LPS group

FA (Fig. 8a). We investigated SNAP-23 protein expression using immunofluorescence staining in the LPS-treated mouse hippocampus and found a reduction in the expression level of the synaptic marker SNAP-23 in the LPS-treated mouse hippocampus compared to the saline-treated group. FA treatment significantly ($P < 0.01$) reversed this reduction in the mouse hippocampus (Fig. 8b). We concluded that FA treatment regulated LPS-induced synaptic dysfunction via regulation of the TLR4-mediated signaling pathway in the mouse hippocampus.

Ferulic Acid Treatment Rescued Cognitive Deficits in LPS-Treated Mice

Previous studies reported that LPS administration produced deficits in spatial learning and memory in the

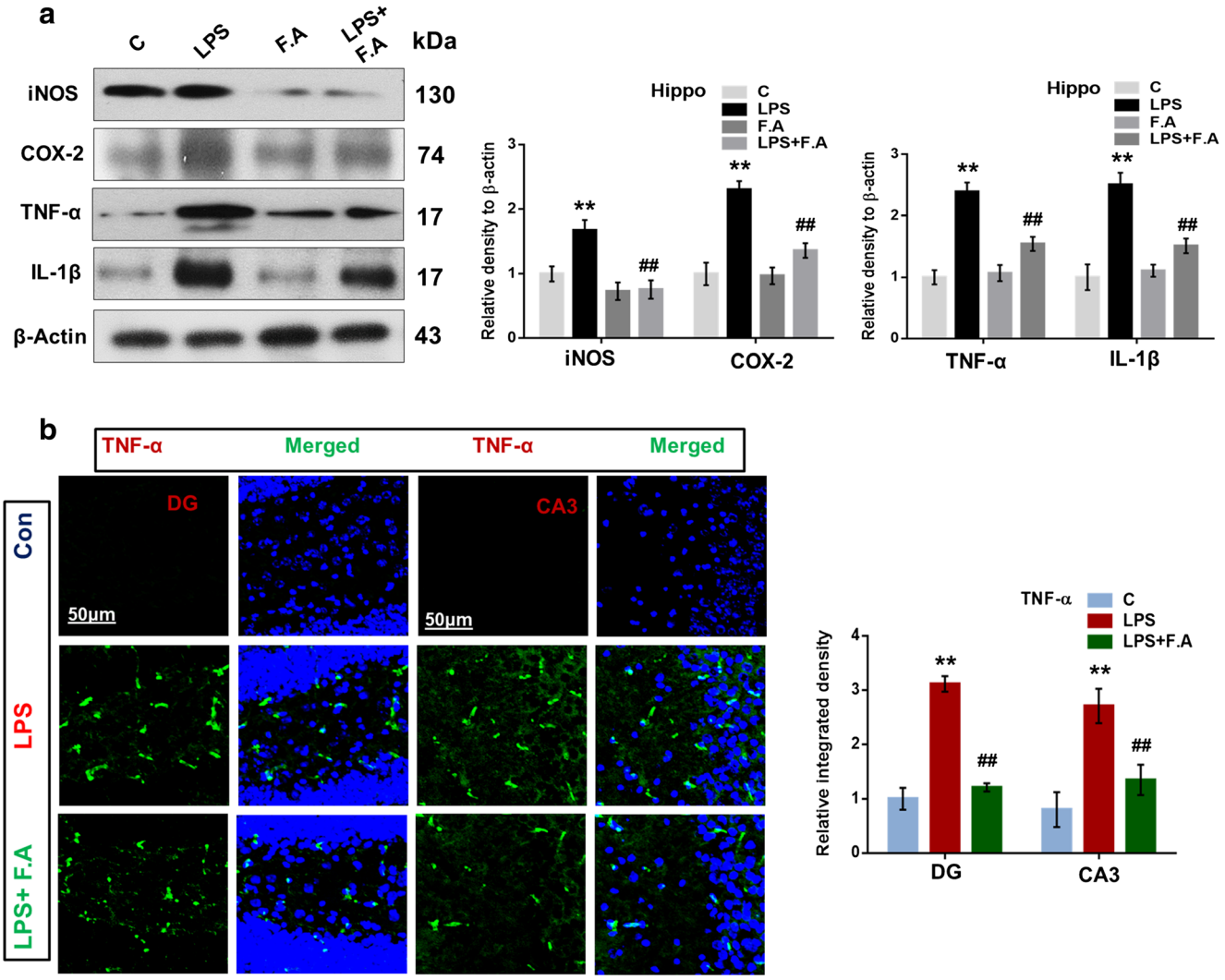

Fig. 6 Ferulic acid inhibited the upregulated expression of iNOS, COX-2, TNF-α, and IL-1β protein in the mouse hippocampus. **a** The expression levels of inflammatory mediators including iNOS, COX-2, TNF-α, and IL-1β were assessed using Western blot analysis in the mouse hippocampus treated with LPS and FA ($n = 8$). In each case, the same immunoblots were probed using β-actin as a loading control. Sigma gel software was used to quantify protein bands. The density values are expressed in arbitrary units (AU) as the mean ± SEM. **b** Representative images of the immunofluorescence staining of TNF-α in the mouse hippocampal CA1 and DG regions of the treated mouse groups ($n = 7$). ImageJ software was used to quantify the immunohistological analysis. Magnification ×10 for immunofluorescence analysis. Statistical analysis was done using one-way ANOVA followed by post hoc analysis. *$P < 0.05$, **$P < 0.01$ vs. control group; #$P < 0.05$, ##$P < 0.01$ vs. LPS group

MWM test [52]. Our study demonstrated that LPS administration for 7 days caused deficits in spatial learning during training days, which was indicated as a longer escape latency to the hidden platform in the LPS-treated mouse groups than the normal saline-treated mice. However, FA treatment significantly improved the spatial learning deficits, which was indicated as a shorter escape latency to the hidden platform in the LPS plus FA-treated mice than the mice treated with LPS alone (Fig. 8c). There was no significant difference in escape latency between the saline-treated mouse groups and the LPS plus FA-treated mouse group. Our findings revealed that FA treatment improved memory performance in LPS-treated mice. We examined the latency to the platform on day 5. Our results demonstrated a longer latency in the LPS-treated mouse group than the saline-treated mice, which was significantly ($P < 0.05$) reduced in the LPS plus FA-treated mice (Fig. 8d). The LPS-treated mouse group exhibited spatial memory deficits, which was demonstrated by the shorter time spent in the target quadrant and the fewer platform crossings during the probe trial on day 5 compared to the saline-treated group. Notably, FA treatment reversed the effects and significantly ($P < 0.05$) increased the number of crossings and time spent in the target quadrants, which indicates that FA treatment improved spatial learning and memory in the LPS-treated mouse group via modulation of microglia-induced neuroinflammation in the mouse hippocampus (Fig. 8e, f).

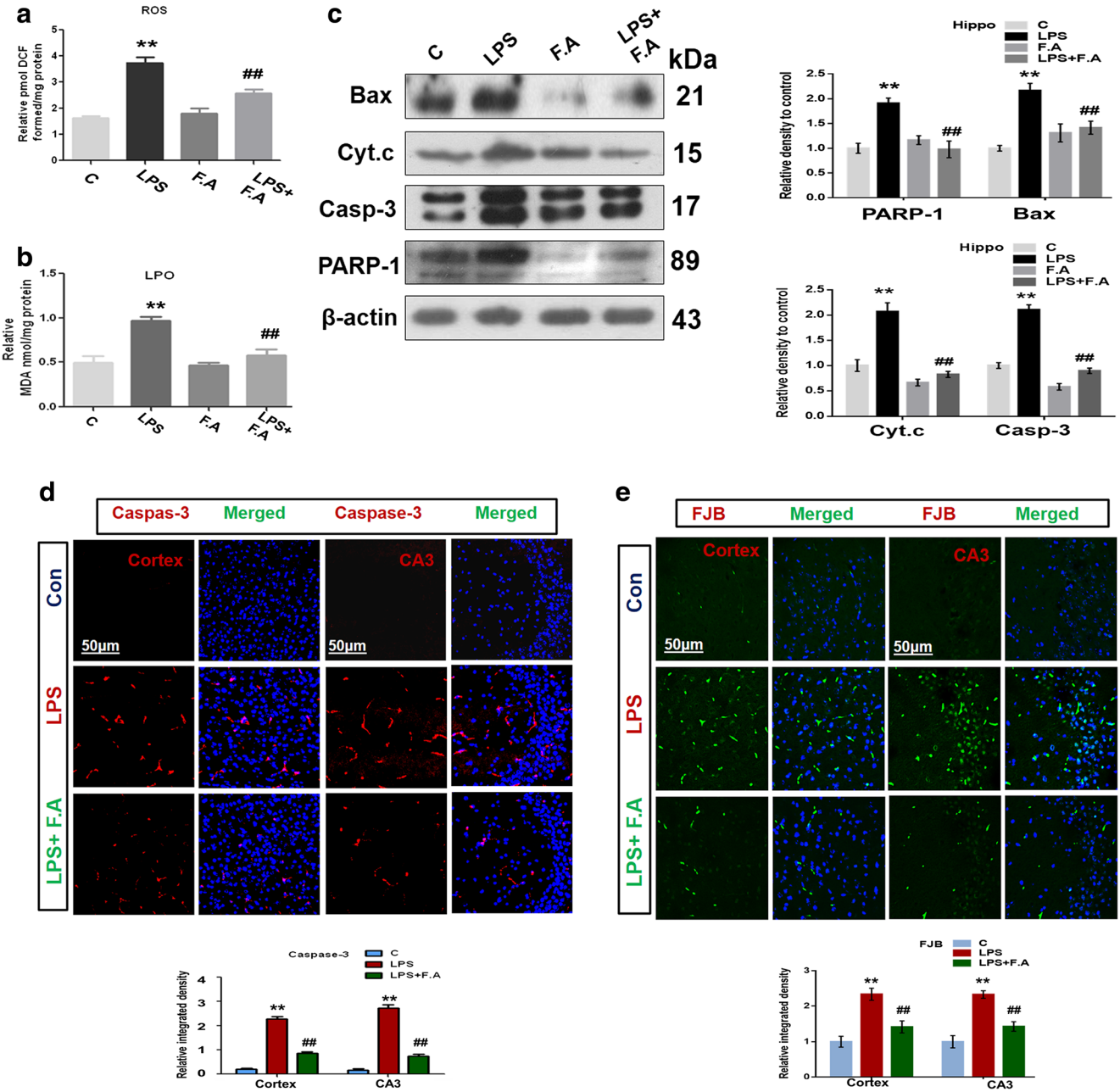

Fig. 7 Ferulic acid reduced LPS-induced oxidative stress and the mitochondrial apoptotic pathway in the LPS-treated mouse hippocampus. **a** Representative histogram for the ROS level. **b** Histogram represents the LPO level in the treated groups. **c** Representative Western blots and histograms for cytochrome C, caspase-3, PARP-1, and Bax in the LPS- and FA-treated groups in the mouse hippocampus ($n = 8$). **d** Representative images of the immunofluorescence staining of caspase-3 in the cortex and CA3 region of the hippocampus ($n = 7$). **e** Confocal microscopic images represent FJB-positive neuronal cells (dead cells) in the cortex and CA3 region of the treated groups. For immunoblot analysis, β-actin was used as a loading control. Bands were quantified using Sigma gel software. ImageJ software was used to quantify the images. Magnification ×10. Values are expressed in arbitrary units (AU) as the mean ± SEM. Statistical analysis was done using one-way ANOVA followed by post hoc analysis. $^{**}P < 0.01$ vs. control group; $^{\#\#}P < 0.01$ vs. LPS group

Discussion

Neuroinflammation is characterized by an abnormal stimulation of microglia in the central nervous system. These cells secrete various inflammatory mediators and increase oxidative stress, which eventually leads to neurological abnormalities in the brain [53, 54]. Therefore, the inhibition of microglia and secreted mediators may be potential therapeutic targets to attenuate neuronal cell death. Our study demonstrated that FA exhibited an inhibitory effect on neuronal cell death in LPS-stimulated microglia via the TLR4-mediated JNK/NF_KB signaling pathway in the mouse hippocampus and

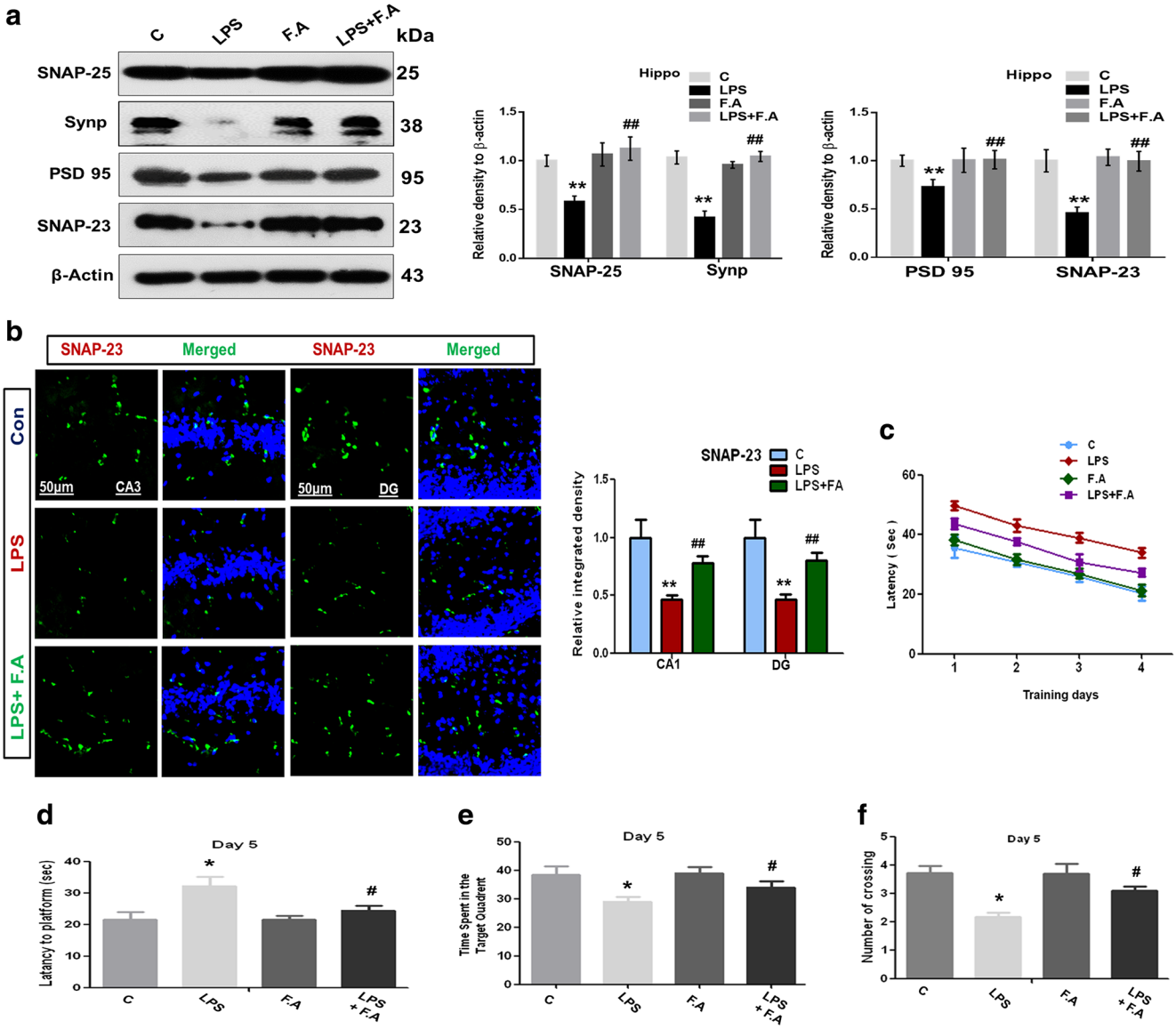

Fig. 8 Ferulic acid treatment reversed LPS-induced deregulation of synaptic markers and memory impairment in mice. **a** The immunoblots and histograms of synaptic markers including PSD-95, synaptophysin, SNAP-25, and SNAP-23 in the LPS- and FA-treated mouse hippocampus. In each case, the same immunoblots were probed using β-actin as a loading control. Sigma gel software was used to quantify the bands. **b** Representative images of the immunofluorescence staining of SNAP-23 in the CA1 and DG regions of the hippocampus ($n = 7$). ImageJ software was used for the quantification of the immunohistological analysis. Magnification ×10. Behavioral deficits were assessed using the MWM test. **c** Representative histogram of the mean escape latency(ies) during training days. **d** Comparative histogram analysis of the latencies to the platform on day 5. **e** Comparison of the time spent in the target quadrant on day 5. **f** Histogram of the number of hidden platform crossings on day 5. Statistical analysis was done using one-way ANOVA followed by post hoc analysis. Values are expressed in arbitrary units (AU) as the mean ± SEM. $^{**}P < 0.01$ vs. control group; $^{\#\#}P < 0.01$ vs. LPS group

BV2 microglial cells. FA reversed the inflammation-induced neuronal degeneration and memory deficits in LPS-treated mouse brains.

Thirteen murine and 11 human TLRs play an important role in immune responses [9, 55]. TLR4 is an important member of the TLR family and was extensively studied. TLR4 is expressed on microglia and macrophages that recognize LPS on gram-negative bacteria [12]. LPS binds to TLR4 and initiates microglia cell activation [22]. TLR4 expression was upregulated in BV2 microglia cells after 24 h of LPS stimulation [56].

TLR4-mediated IKK-NF_KB-JNK activation is a well-recognized signaling pathway in inflammatory responses [57, 58]. The present study demonstrated that LPS administration activated glial cells in the mouse hippocampus, and FA treatment significantly reduced glial cell activation. An inhibitory effect of FA on active astrocytes and microglia was reported in APP/PS1 mice [59]. A recent study demonstrated

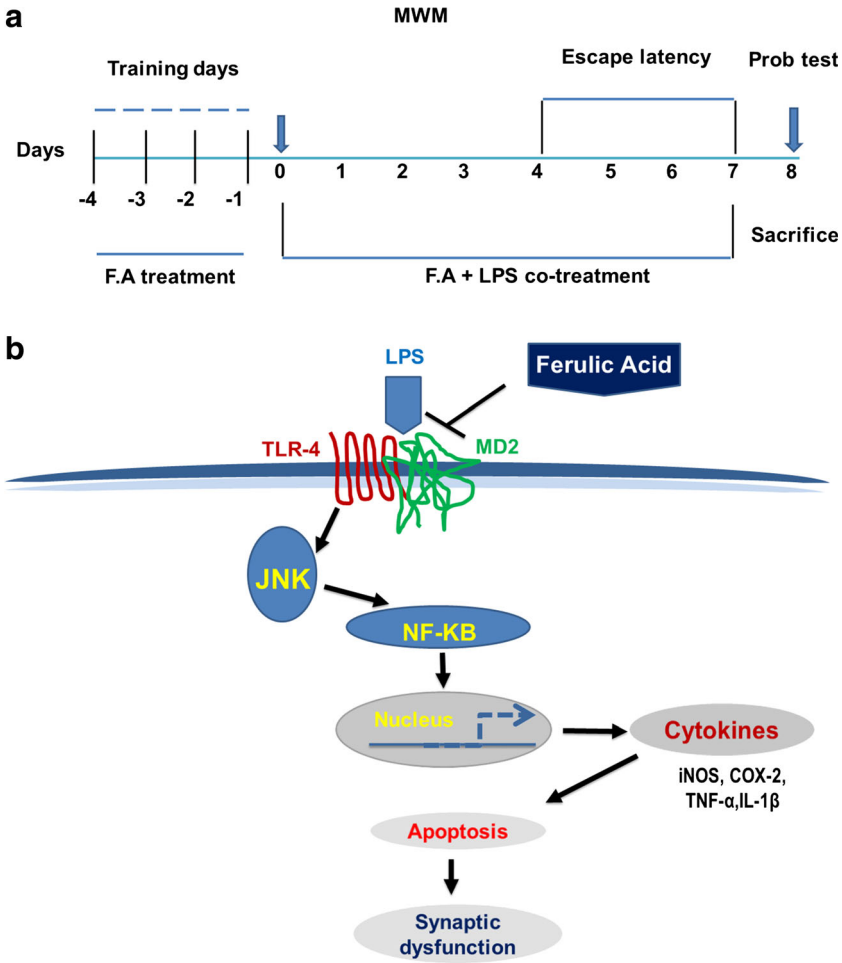

Fig. 9 Treatment schedule and proposed schematic diagram of ferulic acid neuroprotection against LPS-induced neuroinflammation in mouse model. **a** The treatment schedule of FA and LPS treatment in animals. **b** Schematic diagram represents the proposed mechanism of neuroprotection by FA against LPS-induced TLR4 activation and the downstream signaling pathway in mice brain

that TLR4 triggered an inflammatory response via activation of NF_KB [60]. IKKβ phosphorylation leads to the activation of NF_KB and its nuclear translocation [61]. Therefore, we examined the hippocampal levels of TLR4 activation, p-IKKβ and p-NF_KB, which exhibited increased expression in response to LPS treatment. FA treatment significantly abrogated these effects. We examined the predicted binding of FA with TLR4 using molecular docking simulation to further investigate whether the inhibitory effects of FA involved direct interaction of the TLR4. Our results demonstrated that FA targeted the crucial binding site of TLR4 and disrupted TLR4-MD2 complex formation. Previous studies confirmed the involvement TLR4 in association with MD2 for LPS physiological recognition [8, 9]. We observed an increase in JNK phosphorylation in the LPS-treated mouse hippocampus, and FA treatment significantly reduced this increase. A recent study reported that FA exerted anti-inflammatory activity in the RAW264.7 cell line stimulated with LPS via inhibition of iNOS, TNF-α, and IL-6 [62]. The present study investigated inflammatory mediators, including p-JNK, p-NF_KB, iNOS, and TNF-α, in LPS-treated BV2 cells. FA exerted obviously inhibitory effects at two different concentrations, which is consistent with a previous report [63]. TRL4 activation following LPS stimulation activated the IKK complex. This complex phosphorylate IkB is degraded to allow the nuclear translocation of NF_KB [64, 65]. The TLR4 inhibitor TAK-242 was used in LPS-stimulated BV2 cells to elucidate the mechanism of the TLR4-mediated inflammatory response. Our results clearly demonstrated that TAK-242 inhibited LPS-induced TLR4 activation and p-JNK and p-NF_KB, which suggests an antagonistic effect against LPS-evoked TLR4 and downstream signaling molecules. FA treatment exerted similar effects against TLR4 activation and downstream signaling molecules in LPS-treated microglia cells. Several studies reported that MAPK regulated NF_KB-dependent gene transcription. LPS-treated BV2 cells were treated with a JNK-specific inhibitor (SP600125) and FA to elucidate whether JNK regulated NF_KB activation and the possible regulatory effects of FA. SP600125 inhibited JNK activation and regulated NF_KB activation in microglia cells. FA treatment also regulated NF_KB phosphorylation via a JNK-dependent mechanism. We evaluated inflammatory mediators in the LPS-treated mouse hippocampus and the possible reversal effects of FA. Our results demonstrated enhanced inflammatory mediator production in the LPS-treated mouse

hippocampus, and FA obviously inhibited the production of these inflammatory mediators.

Neuroinflammation and oxidative stress are the critical hallmarks of neuronal cell apoptosis. Several studies reported LPS-induced neuronal apoptosis in animal models [66, 67]. Our data clearly demonstrated that LPS treatment induced neuronal apoptosis in the mouse hippocampus via microglia activation. We observed increased expression of Bax, cytochrome C release, cleaved caspase-3, and the DNA damage marker (PARP1) in the mouse hippocampus. Notably, FA treatment attenuated the expression of mitochondrial apoptotic markers and significantly reversed the LPS-induced neuronal disabilities in the mouse hippocampus.

Overactivation of microglia and ROS generation are closely interrelated, and the overactivation of microglia is widely accepted as a major hallmark of ROS generation in the CNS [22, 68]. Intercellular ROS generation leads to the release of inflammatory mediators via MAPKs and NF_KB signaling molecules in microglia [69]. ROS and MDA levels were significantly increased in the LPS-treated mouse hippocampus in the present study, and FA treatment significantly attenuated these increases. Microglia-derived elevations in free radical generation damage neuronal cells, which is implicated in neurodegeneration [70]. Recent studies demonstrated the antioxidant effects of FA in cell lines and animal models [71–73].

Balancing of the neuroinflammatory and antioxidant capacities, reversal of neuronal apoptosis, and reduction in cytokine production by FA may improve the functional survival of hippocampal neurons following LPS-induced cytokine production and oxidative stress. Cytokines greatly impact behavioral abnormalities associated with emotional and anxiety-related behaviors [74, 75]. Hippocampal neuronal function was damaged in LPS-treated mice, which was indicated in the decreased expression of the synaptic markers. FA significantly reversed these effects.

In conclusion, we provide the first evidence that FA inhibits LPS-induced neuroinflammation in the mouse brain via regulation of JNK/NF_KB and TLR4 inhibition. We confirmed that FA interfered with the crucial TLR4 complex to prevent the downstream inflammatory signaling using docking simulation. Whether FA treatment inhibited TLR4 and/or regulated TRL4-dependent JNK/p-NF_KB inhibition is not known. Therefore, further study is needed to elucidate the exact mechanism of FA action. Taken together, these data suggest that FA exerted neuroprotective properties via regulation of neuroinflammation and may have promising therapeutic potential against neuroinflammation-induced neurodegeneration and cognitive deficits in Alzheimer's and Parkinson's diseases.

Acknowledgments This research work was supported by the Brain Research Program through the National Research Foundation of Korea funded by the Ministry of Science, ICT (2016M3C7A1904391).

Compliance with Ethical Standards

All the experiments and animal experimental procedures were approved (Approval ID 125) by the animal ethics committee (IACUC) of the Division of Life Science, Department of Biology, Gyeongsang National University, Republic of South Korea. All the animals were carefully handled and acclimatized for 2 weeks before starting the experimental procedure as according to the animal ethics committee (IACUC) of the Division of Life Science, Department of Biology, Gyeongsang National University, Republic of South Korea.

Conflict of Interest The authors declare that they have no conflict of interest.

References

1. Jha MK, Jeon S, Suk K (2012) Glia as a link between neuroinflammation and neuropathic pain. Immune Netw 12(2):41–47
2. Lee YJ, Choi DY, Choi IS, Kim KH, Kim YH, Kim HM, Lee K, Cho WG et al (2012) Inhibitory effect of 4-O-methylhonokiol on lipopolysaccharide-induced neuroinflammation, amyloidogenesis and memory impairment via inhibition of nuclear factor-kappaB in vitro and in vivo models. J Neuroinflammation 9:35. https://doi.org/10.1186/1742-2094-9-35
3. Dohi K, Ohtaki H, Nakamachi T, Yofu S, Satoh K, Miyamoto K, Song D, Tsunawaki S et al (2010) Gp91phox (NOX2) in classically activated microglia exacerbates traumatic brain injury. J Neuroinflammation 7:41. https://doi.org/10.1186/1742-2094-7-41
4. Wang X, Wang C, Wang J, Zhao S, Zhang K, Wang J, Zhang W, Wu C et al (2014) Pseudoginsenoside-F11 (PF11) exerts anti-neuroinflammatory effects on LPS-activated microglial cells by inhibiting TLR4-mediated TAK1/IKK/NF-kappaB, MAPKs and Akt signaling pathways. Neuropharmacology 79:642–656. https://doi.org/10.1016/j.neuropharm.2014.01.022
5. Yuan L, Liu S, Bai X, Gao Y, Liu G, Wang X, Liu D, Li T et al (2016) Oxytocin inhibits lipopolysaccharide-induced inflammation in microglial cells and attenuates microglial activation in lipopolysaccharide-treated mice. J Neuroinflammation 13(1):77. https://doi.org/10.1186/s12974-016-0541-7
6. Carrasco E, Casper D, Werner P (2007) PGE(2) receptor EP1 renders dopaminergic neurons selectively vulnerable to low-level oxidative stress and direct PGE(2) neurotoxicity. J Neurosci Res 85(14):3109–3117
7. Jara JH, Singh BB, Floden AM, Combs CK (2007) Tumor necrosis factor alpha stimulates NMDA receptor activity in mouse cortical neurons resulting in ERK-dependent death. J Neurochem 100(5):1407–1420
8. Lehnardt S, Lachance C, Patrizi S, Lefebvre S, Follett PL, Jensen FE, Rosenberg PA, Volpe JJ et al (2002) The toll-like receptor TLR4 is necessary for lipopolysaccharide-induced oligodendrocyte injury in the CNS. J Neurosci 22(7):2478–2486
9. Shimazu R, Akashi S, Ogata H, Nagai Y, Fukudome K, Miyake K, Kimoto M (1999) MD-2, a molecule that confers lipopolysaccharide responsiveness on toll-like receptor 4. J Exp Med 189(11):1777–1782
10. Cheong MH, Lee SR, Yoo HS, Jeong JW, Kim GY, Kim WJ, Jung IC, Choi YH (2007) Anti-inflammatory effects of Polygala tenuifolia root through inhibition of NF-kappaB activation in lipopolysaccharide-induced BV2 microglial cells. J Ethnopharmacol 37(3):1402–1408. https://doi.org/10.1016/j.jep.2011.08.008
11. Xie Z, Smith CJ, Van Eldik LJ (2004) Activated glia induce neuron death via MAP kinase signaling pathways involving JNK and p38. Glia 45(2):170–179

12. Glass CK, Saijo K, Winner B, Marchetto MC, Gage FH (2010) Mechanisms underlying inflammation in neurodegeneration. Cell 140(6):918–934. https://doi.org/10.1016/j.cell.2010.02.016
13. Mrak RE, Griffin WS (2005) Glia and their cytokines in progression of neurodegeneration. Neurobiol Aging 26(3):349–354
14. Van Eldik LJ, Thompson WL, Ralay Ranaivo H, Behanna HA, Martin Watterson D (2007) Glia proinflammatory cytokine upregulation as a therapeutic target for neurodegenerative diseases: function-based and target-based discovery approaches. Int Rev Neurobiol 82:277–296
15. Yirmiya R, Goshen I (2011) Immune modulation of learning, memory, neural plasticity and neurogenesis. Brain Behav Immun 25(2): 181–213
16. Bachstetter AD, Xing B, de Almeida L, Dimayuga ER, Watterson DM, Van Eldik LJ (2011) Microglial p38alpha MAPK is a key regulator of proinflammatory cytokine up-regulation induced by toll-like receptor (TLR) ligands or beta-amyloid (Abeta). J Neuroinflammation 8:79
17. Wilms H, Sievers J, Rickert U, Rostami-Yazdi M, Mrowietz U, Lucius R (2010) Dimethylfumarate inhibits microglial and astrocytic inflammation by suppressing the synthesis of nitric oxide, IL-1beta, TNF-alpha and IL-6 in an in-vitro model of brain inflammation. J Neuroinflammation 7:30. https://doi.org/10.1186/1742-2094-7-30
18. Choi Y, Lee MK, Lim SY, Sung SH, Kim YC (2009) Inhibition of inducible NO synthase, cyclooxygenase-2 and interleukin-1beta by torilin is mediated by mitogen-activated protein kinases in microglial BV2 cells. Br J Pharmacol 156(6):933–940. https://doi.org/10.1111/j.1476-5381.2009.00022.x
19. Wang MJ, Huang HY, Chen WF, Chang HF, Kuo JS (2010) Glycogen synthase kinase-3beta inactivation inhibits tumor necrosis factor-alpha production in microglia by modulating nuclear factor kappaB and MLK3/JNK signaling cascades. J Neuroinflammation 7:99. https://doi.org/10.1186/1742-2094-7-99
20. Jang SI, Kim HJ, Kim YJ, Jeong SI, You YO (2006) Tanshinone IIA inhibits LPS-induced NF-kappaB activation in RAW 264.7 cells: possible involvement of the NIK-IKK, ERK1/2, p38 and JNK pathways. Eur J Pharmacol 542(1–3):1–7
21. Vesely MD, Kershaw MH, Schreiber RD, Smyth MJ (2011) Natural innate and adaptive immunity to cancer. Annu Rev Immunol 29: 235–271
22. Block ML, Zecca L, Hong JS (2007) Microglia-mediated neurotoxicity: uncovering the molecular mechanisms. Nat Rev Neurosci 8(1):57–69
23. Zeng KW, Fu H, Liu GX, Wang XM (2010) Icariin attenuates lipopolysaccharide-induced microglial activation and resultant death of neurons by inhibiting TAK1/IKK/NF-kappaB and JNK/p38 MAPK pathways. Int Immunopharmacol 10(6):668–678. https://doi.org/10.1016/j.intimp.2010.03.010
24. Barone E, Calabrese V, Mancuso C (2009) Ferulic acid and its therapeutic potential as a hormetin for age-related diseases. Biogerontology 10(2):97–108
25. Zhao Z, Moghadasian MH (2008) Chemistry, natural sources, dietary intake and pharmacokinetic properties of ferulic acid: a review. Food Chem 109(4):691–702. https://doi.org/10.1016/j.foodchem.2008.02.039
26. Cheng CY, Su SY, Tang NY, Ho TY, Chiang SY, Hsieh CL (2008) Ferulic acid provides neuroprotection against oxidative stress-related apoptosis after cerebral ischemia/reperfusion injury by inhibiting ICAM-1 mRNA expression in rats. Brain Res 1209:136–150
27. Kim HS, Cho JY, Kim DH, Yan JJ, Lee HK, Suh HW, Song DK (2004) Inhibitory effects of long-term administration of ferulic acid on microglial activation induced by intracerebroventricular injection of beta-amyloid peptide (1-42) in mice. Biol Pharm Bull 27: 120–121
28. Sultana R (2012) Ferulic acid ethyl ester as a potential therapy in neurodegenerative disorders. Biochim Biophys Acta 1822(5):748–752. https://doi.org/10.1016/j.bbadis.2011.10.015
29. Yan JJ, Cho JY, Kim HS, Kim KL, Jung JS, Huh SO, Suh HW, Kim YH et al (2001) Protection against beta-amyloid peptide toxicity in vivo with long-term administration of ferulic acid. Br J Pharmacol 133(1):89–96
30. Shah SA, Yoon GH, Chung SS, Abid MN, Kim TH, Lee HY, Kim MO (2017) Novel osmotin inhibits SREBP2 via the AdipoR1/AMPK/SIRT1 pathway to improve Alzheimer's disease neuropathological deficits. Mol Psychiatry 22(3):407–416
31. Shah SA, Amin FU, Khan M, Abid MN, Rehman SU, Kim TH, Kim MW, Kim MO (2016) Anthocyanins abrogate glutamate-induced AMPK activation, oxidative stress, neuroinflammation, and neurodegeneration in postnatal rat brain. J Neuroinflammation 13(1):286
32. Rehman SU, Shah SA, Ali T, Chung JI, Kim MO (2016) Anthocyanins reversed D-galactose-induced oxidative stress and Neuroinflammation mediated cognitive impairment in adult rats. Mol Neurobiol 54(1):255–271
33. Verdonk ML, Cole JC, Hartshorn MJ, Murray CW, Taylor RD (2003) Improved protein-ligand docking using GOLD. Proteins 52(4):609–623
34. Kim HM, Park BS, Kim JI, Kim SE, Lee J, Oh SC, Enkhbayar P, Matsushima N et al (2007) Crystal structure of the TLR4-MD-2 complex with bound endotoxin antagonist Eritoran. Cell 130(5): 906–917
35. Berman HM, Westbrook J, Feng Z, Gilliland G, Bhat TN, Weissig H, Shindyalov IN, Bourne PE (2000) The protein data bank. Nucleic Acid Res 28(1):235–242
36. Park BS, Song DH, Kim BS, Lee H, Lee JO (2009) The structural basis of lipopolysaccharide recognition by the TLR4-MD-2 complex. Nature 458:1191–1195
37. Han J., Kim H. J., Lee S. C., Hong S., Park K., Jeon Y. H., Kim D., Cheong H. K., Kim H. S Structure-based rational design of a Toll-like receptor 4 (TLR4) decoy receptor with high binding affinity for a target protein. PloS ONE 7(2):e30929.
38. Li Y, Han L, Liu Z, Wang R (2014) Comparative assessment of scoring functions on an updated benchmark: 2. Evaluation methods and general results. J Chem Inf Model 54(6):1717–1736. https://doi.org/10.1021/ci500081m
39. Ni H, Zhao W, Kong X, Li H, Ouyang J (2014) Celastrol inhibits lipopolysaccharide-induced angiogenesis by suppressing TLR4-triggered nuclear factor-kappa B activation. Acta Haematol 131(2):102–111
40. Matzinger P (2002) The danger model: a renewed sense of self. Science 296(5566):301–305
41. Svajger U, Brus B, Turk S, Sova M, Hodnik V, Anderluh G, Gobec S (2013) Novel toll-like receptor 4 (TLR4) antagonists identified by structure- and ligand-based virtual screening. Eur J Med Chem 70: 393–399. https://doi.org/10.1016/j.ejmech.2013.10.019
42. Verstak B, Nagpal K, Bottomley SP, Golenbock DT, Hertzog PJ, Mansell A (2009) MyD88 adapter-like (mal)/TIRAP interaction with TRAF6 is critical for TLR2- and TLR4-mediated NF-kappaB proinflammatory responses. J Biol Chem 284(36):24192–24203
43. Zhang L, Wu C, Zhao S, Yuan D, Lian G, Wang X, Wang L, Yang J (2010) Demethoxycurcumin, a natural derivative of curcumin attenuates LPS-induced pro-inflammatory responses through down-regulation of intracellular ROS-related MAPK/NF-kappaB signaling pathways in N9 microglia induced by lipopolysaccharide. Int Immunopharmacol 10(3):331–338. https://doi.org/10.1016/j.intimp.2009.12.004
44. Roy A, Jana A, Yatish K, Freidt MB, Fung YK, Martinson JA, Pahan K (2008) Reactive oxygen species up-regulate CD11b in microglia via nitric oxide: implications for neurodegenerative diseases. Free Radic Biol Med 45(5):686–699

45. Debatin KM, Poncet D, Kroemer G (2002) Chemotherapy: targeting the mitochondrial cell death pathway. Oncogene 21(57): 8786–8803
46. Brown GC, Neher JJ (2010) Inflammatory neurodegeneration and mechanisms of microglial killing of neurons. Mol Neurobiol 41(2–3):242–247
47. Li D, Li X, Wu J, Li J, Zhang L, Xiong T, Tang J, Qu Y et al (2015) Involvement of the JNK/FOXO3a/Bim pathway in neuronal apoptosis after hypoxic-ischemic brain damage in neonatal rats. PLoS One 10(7):e0132998. https://doi.org/10.1371/journal.pone.0132998
48. Fruhauf PK, Ineu RP, Tomazi L, Duarte T, Mello CF, Rubin MA (2015) Spermine reverses lipopolysaccharide-induced memory deficit in mice. J Neuroinflammation 12:3. https://doi.org/10.1186/s12974-014-0220-5
49. Nakajima K, Kohsaka S (1998) Functional roles of microglia in the central nervous system. Hum Cell 11(3):141–155
50. Czerniawski J, Miyashita T, Lewandowski G, Guzowski JF (2015) Systemic lipopolysaccharide administration impairs retrieval of context-object discrimination, but not spatial, memory: evidence for selective disruption of specific hippocampus-dependent memory functions during acute neuroinflammation. Brain Behav Immun 44:159–166. https://doi.org/10.1016/j.bbi.2014.09.014
51. Gabellec MM, Griffais R, Fillion G, Haour F (1995) Expression of interleukin 1 alpha, interleukin 1 beta and interleukin 1 receptor antagonist mRNA in mouse brain: regulation by bacterial lipopolysaccharide (LPS) treatment. Brain Res Mol Brain Res 31(1–2):122–130
52. Badshah H, Ali T, Rehman S-U, Faiz-ul A, Ullah F, Kim TH, Kim MO (2016) Protective effect of lupeol against lipopolysaccharide-induced neuroinflammation via the p38/c-Jun N-terminal kinase pathway in the adult mouse brain. J Neuroimmune Pharmacol 11:48–60
53. Agostinho P, Cunha RA, Oliveira C (2010) Neuroinflammation, oxidative stress and the pathogenesis of Alzheimer's disease. Curr Pharm Des 16(25):2766–2778
54. Dai JN, Zong Y, Zhong LM, Li YM, Zhang W, Bian LG, Ai QL, Liu YD et al (2011) Gastrodin inhibits expression of inducible NO synthase, cyclooxygenase-2 and proinflammatory cytokines in cultured LPS-stimulated microglia via MAPK pathways. PLoS One 6(7):e21891. https://doi.org/10.1371/journal.pone.0021891
55. Aravalli RN, Peterson PK, Lokensgard JR (2007) Toll-like receptors in defense and damage of the central nervous system. J NeuroImmune Pharmacol 2(4):297–312
56. Yoon HM, Jang KJ, Han MS, Jeong JW, Kim GY, Lee JH, Choi YH (2013) Ganoderma lucidum ethanol extract inhibits the inflammatory response by suppressing the NF-kappaB and toll-like receptor pathways in lipopolysaccharide-stimulated BV2 microglial cells. Exp Ther Med 5(3):957–963
57. Doyle SL, O'Neill LA (2006) Toll-like receptors: from the discovery of NFkappaB to new insights into transcriptional regulations in innate immunity. Biochem Pharmacol 72(9):1102–1113
58. Liu S, Kielian T (2009) Microglial activation by Citrobacter koseri is mediated by TLR4- and MyD88-dependent pathways. J Immunol 183(9):5537–5547. https://doi.org/10.4049/jimmunol.0900083
59. Mori T, Koyama N, Guillot-Sestier MV, Tan J, Town T (2013) Ferulic acid is a nutraceutical beta-secretase modulator that improves behavioral impairment and alzheimer-like pathology in transgenic mice. PLoS One 8(2):e55774. https://doi.org/10.1371/journal.pone.0055774
60. Kuper C, Beck FX, Neuhofer W (2012) Toll-like receptor 4 activates NF-kappaB and MAP kinase pathways to regulate expression of proinflammatory COX-2 in renal medullary collecting duct cells. Am J Physiol Renal Physiol 302(1):F38–F46. https://doi.org/10.1152/ajprenal.00590.2010
61. Perkins ND (2007) Integrating cell-signalling pathways with NF-kappaB and IKK function. Nat Rev Mol Cell Biol 8(1):49–62
62. Lampiasi N, Montana G (2016) The molecular events behind ferulic acid mediated modulation of IL-6 expression in LPS-activated Raw 264.7 cells. Immunobiology 221(3):486–493
63. Koshiguchi M, Komazaki H, Hirai S, Egashira Y (2017) Ferulic acid suppresses expression of tryptophan metabolic key enzyme indoleamine 2, 3-dioxygenase via NFκB and p38 MAPK in lipopolysaccharide-stimulated microglial cells. Biosci Biotechnol Biochem 81(5):966–971. https://doi.org/10.1080/09168451.2016.1274636
64. Gatheral T, Reed DM, Moreno L, Gough PJ, Votta BJ, Sehon CA, Rickard DJ, Bertin J et al (2015) A key role for the endothelium in NOD1 mediated vascular inflammation: comparison to TLR4 responses. PLoS One 7(8):e42386. https://doi.org/10.1371/journal.pone.0042386
65. Kim IT, Ryu S, Shin JS, Choi JH, Park HJ, Lee KT (2012) Euscaphic acid isolated from roots of Rosa rugosa inhibits LPS-induced inflammatory responses via TLR4-mediated NF-κB inactivation in RAW 264.7 macrophages. J Cell Biochem 113(6):1936–1946. https://doi.org/10.1002/jcb.24062
66. Nikseresht S, Khodagholi F, Nategh M, Dargahi L (2015) RIP1 inhibition rescues from LPS-induced RIP3-mediated programmed cell death, distributed energy metabolism and spatial memory impairment. J Mol Neurosci 57(2):219–230. https://doi.org/10.1007/s12031-015-0609-3
67. Santhanasabapathy R, Sudhandiran G (2015) Farnesol attenuates lipopolysaccharide-induced neurodegeneration in Swiss albino mice by regulating intrinsic apoptotic cascade. Brain Res 1620: 42–56. https://doi.org/10.1016/j.brainres.2015.04.043
68. Sorce S, Krause KH (2009) NOX enzymes in the central nervous system: from signaling to disease. Antioxid Redox Signal 11(10): 2481–2504. https://doi.org/10.1089/ARS.2009.2578
69. Pan XD, Chen XC, Zhu YG, Zhang J, Huang TW, Chen LM, Ye QY, Huang HP (2008) Neuroprotective role of tripchlorolide on inflammatory neurotoxicity induced by lipopolysaccharide-activated microglia. Biochem Pharmacol 76(3):362–372. https://doi.org/10.1016/j.bcp.2008.05.018
70. Parvathenani LK, Tertyshnikova S, Greco CR, Roberts SB, Robertson B, Posmantur R (2003) P2X7 mediates superoxide production in primary microglia and is up-regulated in a transgenic mouse model of Alzheimer's disease. J Biol Chem 278(15): 13309–13317
71. Catino S, Paciello F, Miceli F, Rolesi R, Troiani D, Calabrese V, Santangelo R, Mancuso C (2015) Ferulic acid regulates the Nrf2/heme oxygenase-1 system and counteracts trimethyltin-induced neuronal damage in the human neuroblastoma cell line SH-SY5Y. Front Pharmacol 6:305. https://doi.org/10.3389/fphar.2015.00305
72. Shen Y, Zhang H, Wang L, Qian H, Qi Y, Miao X, Cheng L, Qi X (2016) Protective effect of ferulic acid against 2,2′-azobis(2-amidinopropane) dihydrochloride-induced oxidative stress in PC12 cells. Cell Mol Biol (Noisy-le-grand) 62(1):109–116
73. Tsai FS, Wu LY, Yang SE, Cheng HY, Tsai CC, Wu CR, Lin LW (2015) Ferulic acid reverses the cognitive dysfunction caused by amyloid beta peptide 1-40 through anti-oxidant activity and cholinergic activation in rats. Am J Chin Med 43(2):319–335. https://doi.org/10.1142/S0192415X15500214
74. Reader BF, Jarrett BL, McKim DB, Wohleb ES, Godbout JP, Sheridan JF (2015) Peripheral and central effects of repeated social defeat stress: monocyte trafficking, microglial activation, and anxiety. Neuroscience 289:429–442. https://doi.org/10.1016/j.neuroscience.2015.01.001
75. Terrando N, Monaco C, Ma D, Foxwell BM, Feldmann M, Maze M (2010) Tumor necrosis factor-alpha triggers a cytokine cascade yielding postoperative cognitive decline. Proc Natl Acad Sci U S A 107(47):20518–20522. https://doi.org/10.1073/pnas.1014557107